3-16-2021

Designing Ionic Liquid-Derived Polymer Composites from Poly(Ionic Liquid)–Ionene Semi-interpenetrating Networks

Kathryn E. O'Harra
University of Alabama - Tuscaloosa

George E. Timmerman
Murray State University

Jason E. Barra
University of Alabama - Tuscaloosa

Kevin Miller
Murray State University, kmiller38@murraystate.edu

Recommended Citation

O'Harra, K. E., Timmermann, G. M., Bara, J. E., & Miller, K. M. (2021). Designing Ionic Liquid-Derived Polymer Composites from Poly (Ionic Liquid)–Ionene Semi-interpenetrating Networks. ACS Applied Polymer Materials. https://doi.org/10.1021/acsapm.1c00080

Designing Ionic Liquid–Derived Polymer Composites from Poly(Ionic Liquid)–Ionene Semi-Interpenetrating Networks

Kathryn E. O'Harra[1], George M. Timmermann[2], Jason E. Bara[1,*], Kevin M. Miller[2,*]

[1]Chemical & Biological Engineering, University of Alabama, Tuscaloosa, AL USA 35487-0203

[2]Department of Chemistry, Murray State University, Murray, KY USA 42071

*Corresponding Authors' email addresses: jbara@eng.ua.edu (J. E. Bara); kmiller38@murraystate.edu (K. M. Miller)

ABSTRACT

While the solvating power of ionic liquids (ILs) for a variety of solute types including polymers is well-known, the use of ILs as solvents for ionenes – charged polymers with cationic moieties within the backbone – has only recently begun to be explored. IL-ionene combinations offer vast possibilities to make iongels and perhaps even use ILs to exert control over ionene organization (i.e., coil or rod). If the IL solvent itself is also polymerizable, then poly(IL)-ionene semi-interpenetrating networks (semi-IPNs) can be achieved. This manuscript reports, for the first time, examples of poly(IL)-ionene semi-IPNs formed by dissolving an ionene in a vinyl-functionalized imidazolium IL followed by subsequent photopolymerization of the IL around the ionene. The resultant poly(IL)-ionene semi-IPNs exhibit greater elasticity and ionic conductivity than the neat poly(IL). Thus, the addition of 10 – 20 wt% ionene can lead to significant changes in the properties of poly(IL) materials. Given the limitless possibilities for IL and ionene structures, this unique type of ionic composite presents vast opportunities for material design.

KEYWORDS: ionene, poly(ionic liquid), interpenetrating network, ionic conductivity, polyamide

INTRODUCTION

Ionic polymers which contain functional groups akin to those associated with ionic liquids (ILs) in the repeating unit represent a diverse class of materials which have been utilized in a wide variety of applications, from solid polymer electrolytes[1-5] and ion-exchange membranes,[6,7] to CO_2 sorbents and gas separation membranes,[8-11] and antimicrobial coatings.[12] The ability to fine-tune the nature of the ionic groups (whether cationic, anionic, zwitterionic) and their spacing and location within the polymer architecture has resulted in a seemingly limitless number of possible designs and end uses. Much of the recent inspiration for the design of IL-derived polymers has been directly related to the large number of tunable, "task-specific" ILs available. Ion-containing polymers can generally can be classified into two groups based upon the location of the covalently bound IL group. Polymerizable ionic liquids or poly(ionic liquid)s (PILs) are ion-containing polymers wherein a pendant ionic liquid (IL) group is present in the repeating unit, and share similarities with classical polyelectrolytes.[1,13-15] Ionenes represent the other sub-class of ion-containing polymers where the ionic group (typically cationic) is covalently bound within the backbone.[16-18]

The most common approach towards the synthesis of PILs is the polymerization of vinyl-, (meth)acrylic- or styrenyl-substituted IL monomers.[13-17,19,20] Ohno and coworkers were the first to comprehensively illustrate how PILs could be made through the polymerization of various imidazolium-functionalized IL monomers.[21-23] From these studies, it was hypothesized that ion transport and conductivity were primarily controlled by the flexibility of the pendant linkage. Several other important works have followed, focusing on the relationship between polymer/ion structure and ionic conductivity. Generally speaking, using large, non-coordinating anions such as bis(trifluoromethylsulfonyl)imide ([NTf_2]) (or other fluorinated anions such as BF_4 and PF_6)

depresses the T_g of the PIL, leading to relatively high ionic conductivity.[24,25] Various pendant groups (alkyl, oligo(ethylene glycol) for example) have been employed to further improve flexibility and ion mobility.[19,26,27] Block copolymer PILs have also been investigated, synthesized using either RAFT or anionic polymerization.[16,28-31] In these systems, the PIL block was found to form conductive microchannels in the presence of a non-ionic block such as polystyrene or poly(methyl methacrylate), leading to relatively high ionic conductivities.

Ionenes prepared from IL-containing monomers are far less common; however, a few excellent reviews have been written which highlight the vast array of step-growth polymerization approaches used.[16-17] The most classical strategy is the use of the Menshutkin (S_N2) reaction between a tertiary diamine,[16,32,33] diphosphine[34] or bisimidazole[17,18,35-38] with an alkyl dihalide (or similar compound). This allows for a great deal of variation in the linker groups (alkyl vs. aromatic for example). Other examples have utilized polyurethane or polyesterification chemistry to achieve linear ionenes.[39-41] Covalently crosslinked, imidazolium-containing ionene networks have also been reported, utilizing Michael addition chemistry or thiol-ene photopolymerization.[42-45]

Ion transport in ion-containing polymers has been related to a number of structural features, including the T_g, molecular weight, water content (humidity) and morphology of the polymer-counterion pair.[30,31,45-47] As PILs are single-ion conductors, the untethered counterion is the primary driving force for conduction, and those that are bulkier and non-coordinating tend to produce higher conduction by increasing free volume, reflected in reduced T_g values, which facilitates ion hopping.[46,48-50] Additional enhancements in ionic conductivity have been observed when longer, more flexible side or linker chains are employed. For example, Long, *et al.* related morphology with ionic conductivity in a series of alkyl-substituted, imidazolium PILs and revealed that larger counteranions with alkyl chains of moderate length led to reduced T_g values and increased conductivities.[48] Other modifications of PIL or ionene architecture have produced interesting microstructures/morphologies while improving ionic conductivity and ion transport. Multi-block PIL copolymers, several examples of which were previously referenced, are prime examples where morphology can be manipulated through structural changes in order to improve ion transport and conductivity.[16,28-31] While there is not a clear, definitive advantage for using a PIL architecture versus an ionene, Segalman *et al.* has demonstrated that utilizing an ionene structure appears to enhance ion mobility as the nanostructure was more ordered.[51] Increased order results in a more "percolated" network of anions throughout the material. Covalently crosslinked ionene networks, when precise control of functional group ratio is achieved, also appear to exhibit a more percolated nature as the network forces anions to disperse more uniformly as supported by X-ray scattering data.[33,45]

Interpenetrating networks (IPN)s are materials where two distinct polymer species (typically networks) coexist through noncovalent physical interactions.[52] The ability of the two polymers to exhibit good miscibility and mechanical stability stems from the effectiveness of their physical entanglements. Semi-interpenetrating networks (semi-IPNs) are similar in terms of their ability to form a uniform material through entanglements; however, one of the polymers involved is not a network and thus can be physically separated.[53] Either of these approaches allows for the combination of desirable attributes between two distinct polymers (i.e. thermal and/or mechanical stability, processability, conductivity, bio-compatibility), creating a hybrid material which exhibits application-specific properties. The use of PILs and ionenes in IPNs and semi-IPNs has been very limited. Vidal and coworkers prepared the first known IPN which involved a PIL network prepared from crosslinking an aryl sulfonate-substituted methacrylate monomer (with imidazolium countercation).[54] The two networks (the PIL and the other a crosslinked, polybutadiene-based polyurethane) were polymerized simultaneously in dimethyl sulfoxide. Dynamic mechanical thermal analysis (DMTA) showed that the resulting IPN exhibited a single, uniform tan δ peak, indicating good miscibility between the two networks. Firestone, *et al.* reported a photopolymerized IPN hydrogel, prepared through the ionic entanglement of two linear PILs (one cationic and the other anionic).[55] X-ray scattering data indicated that the IPN adopted a lamellar structure while thermal analysis data supported the hypothesis that the resulting IPN was homogeneous. Since these initial findings, several other examples of IPNs and semi-IPNs have been reported, with a focus on tailoring the polymers towards specific applications such as gas separation,[56] multi-responsive hydrogels[57,58] and solid-state polymer electrolytes.[59-63] The most conductive networks from this group were found to be on the order of 10^{-4} S/cm at 25 °C.

To continue to meet the demand for high-performance materials with higher ionic conductivities and improved chemical and mechanical stability, researchers must continue to probe the relationships that exist between structural changes, ionic conductivity and ion transport. Herein, we report the synthesis and thermal, mechanical and conductive properties of a series of semi-IPNs wherein an imidazolium PIL network was formed via photopolymerization in the presence of a linear, imidazolium ionene (10-20 wt%). To the best of our knowledge, this is the first example of such a combination where an ionene has been fully dissolved in an IL phase. While a number of works have added ILs to ionenes, particularly for the formation of gas separation membranes, the resulting ionene + IL materials have still been solid composites. Mittenthal, *et al.* showed that the very limited solubility of a polyimide-ionene in an $[C_4mim][NTf_2]$ at 170 °C resulted in the formation of an ionogel when cooled to room temperature, with the bulk of the ionene remaining undissolved.[9] While little is known about the behavior of ionenes in ILs, it is clear that there are potentially endless IL-ionene (i.e. solvent-solute) combinations. If the IL is photopolymerizable, semi-IPNs can be formed where the ionene morphology (i.e. coil, rod) can be altered by simply changing the nature of the IL solvent.

In this work, polyamide-ionenes were prepared from amide-functionalized, bisimidazole monomers inspired by Nylon® chemistry (herein referred to as “AC API”), coupled with various dihalide linkers, resulting in materials with a variety of backbones (flexible and rigid). Differential scanning calorimetry (DSC) and dynamic mechanical analysis (DMA) was utilized to analyze the thermal and mechanical properties of the semi-IPNs, respectively, while anhydrous ionic conductivities, as determined from dielectric relaxation spectroscopy experiments, of up to 10^{-5} S/cm at 20 °C were observed.

EXPERIMENTAL

General: Adipoyl chloride (AC, 98%) was purchased from BeanTown Chemical. 1-(3-Aminopropyl)imidazole (API, > 97%), α,α'-Dichloro-*p*-xylene (*p*DCXy, 98%), potassium carbonate (K_2CO_3) and lithium bis(trifluoromethanesulfonyl)imide ($LiNTf_2$) were purchased from TCI. 1,6-dibromohexane (DiBrHEX, > 97%) and 1,10-dibromodecane (DiBrDEC, 97 %) were purchased from Alfa Aesar. Dichloromethane (DCM, ACS grade), tetrahydrofuran (THF, Anhydrous), diethyl ether (Et_2O, Anhydrous), and *N*-methyl-2-pyrrolidone (NMP, ACS grade) were purchased from VWR. Phenylbis(2,4,6-trimethylbenzoyl)phosphine oxide (TPO, 97%) and trimethylolpropane ethoxylate triacrylate (ETMPTA, Mn ~ 428) were purchased from Aldrich. An ELGA Purelab® Ultra filtration device produced ultrapure water having a resistivity of 18 MΩ-cm.

Synthesis of N1,N6-bis(3-(1*H*-imidazol-1-yl)propyl)adipamide (“AC API”): The amide-functionalized bis-imidazole monomer utilized in this work, “AC API”, was synthesized on a large scale with high yields. K_2CO_3 (95.15 g, 688 mmol) and API (43.09 g, 344 mmol) were added to 500 mL of DI H_2O in a 1.5L IKA batch reactor. Adipoyl chloride (30.00 g, 23.8 mL, 164 mmol) was dissolved in 200 mL DCM, which was added slowly to the stirring aqueous phase. The reactor was equipped with a condenser and was heated at 45 °C for 16 h. The reaction was cooled to RT and transferred to a separatory funnel. Three phases were apparent, including a low organic phase, a middle aqueous phase, and a brown oil top layer. This oil was separated and washed with DI H_2O, then dried under vacuum overnight (43.12 g, 73%). ^{1}H NMR (500 MHz, DMSO-d_6): δ 8.00 – 7.95 (m, 2H), 7.61 (s, 2H), 7.15 (s, 2H), 6.86 (s, 2H), 3.93 (t, J = 6.7 Hz, 4H), 2.98 (q, J = 6.2 Hz, 4H), 2.07 (s, 4H), 1.82 – 1.75 (m, 4H), 1.46 (s, 4H).

Synthesis of [AC API C_6][NTf_2]. AC API (2.50 g, 6.94 mmol) and 1,6-dibromohexane (1.69 g, 6.94 mmol) were added with 40 mL NMP to a 250 mL round-bottom heavy-walled pressure vessel (Ace Glass) equipped with a stir bar. The reaction was heated while stirring for 24 h at 150 °C. The solution was cooled to RT, and poured into DI H_2O with 2.5 eq. of $LiNTf_2$ (4.98 g, 17.3 mmol) to promote anion metathesis. The ionene precipitates as a light brown gel, thus the water layer was decanted and the polymer was dried for 24 h at 100 °C. To clean each ionene and remove oligomeric content, 100 mL of THF was added to the polymer, resulting in a lower oily phase (polymer) and a discolored upper phase (impurities, oligomers) which was decanted. The bottom layer was precipitated in Et_2O to again yield a gel, followed by decanting the Et_2O and drying the ionene overnight at 100 °C (3.87 g, 56%). ^{1}H NMR (500 MHz, DMSO-d_6): δ 9.16 (s, 2H), 7.90 (s, 2H), 7.78 (s, 4H), 4.16 (br, 8H), 3.37 (s, 4H), 3.05 (d, J = 5.5 Hz, 4H), 2.08 – 1.79 (m, 8H), 1.48 – 1.25 (m, 8H).

Synthesis of [AC API C_{10}][NTf_2]. The synthesis of [AC API C_{10}][NTf_2] followed a similar procedure. AC API (2.50 g, 6.94 mmol) and 1,10-dibromodecane (2.08 g, 6.94 mmol) were polymerized in NMP at 150 °C. The polymer was subsequently precipitated in DI H_2O with 2.5 eq. of $LiNTf_2$ (4.98 g, 17.3 mmol), and purified by the same method with a THF wash and reprecipitation in Et_2O. The ionene was dried to yield a brown gel (4.21 g, 58%). ^1H NMR (500 MHz, DMSO-d_6): δ 9.16 (s, 2H), 7.88 (s, 2H), 7.79 (s, 4H), 4.15 (t, J = 6.2 Hz, 8H), 3.37 - 3.31 (dt, J = 6.9 Hz, 6H), 3.04 (q, J = 6.0 Hz, 4H), 2.07 (m, J = 8.0 Hz, 4H), 1.95 – 1.85 (m, 4H), 1.79 (s, 4H), 1.48 - 1.36 (m, 8H).

Synthesis of [AC API pXy][NTf_2]. The synthesis of [AC API pXy][NTf_2] followed a similar procedure. AC API (2.50 g, 6.94 mmol) and pDCX (1.21 g, 6.94 mmol) were polymerized in NMP at 150 °C. The polymer was subsequently precipitated in DI H_2O with 2.5 eq. of $LiNTf_2$ (4.98 g, 17.3 mmol), and purified by the same method with a THF wash and reprecipitation in Et_2O. The ionene was dried to yield a viscous brown gel (5.32 g, 74%). ^1H NMR (500 MHz, DMSO-*d*6): δ 9.27 (d, J = 10.8 Hz, 2H), 7.92 – 7.87 (m, 2H), 7.77 (q, J = 11.5, 9.7 Hz, 4H), 7.52 – 7.39 (m, 4H), 7.36 (d, J = 9.8 Hz, 2H), 5.46 – 5.37 (m, 4H), 4.50 (d, J = 5.9 Hz, 4H), 4.17 (t, J = 6.4 Hz, 4H), 3.07 – 3.03 (m, 2H), 1.91 (dq, J = 15.6, 7.6, 6.7 Hz, 4H), 1.48 (s, 4H).

Semi-IPN Photopolymerization. The synthesis of 1-vinyl-3-butylimidazolium bistriflimide ([C_4vim][NTf_2]) was completed following a published procedure by Pinaud *et al.*[64] In a representative photopolymerization procedure, the photoinitiator diphenyl(2,4,6-trimethylbenzoyl)phosphine oxide (TPO, 6.3 mg, 1 wt-% based upon alkene), ethoxylated trimethyloylpropane triacrylate (ETMPTA, 75.0 mg, 10 wt-% of total mixture), [AC API C_6][NTf_2] (0.16 g, 20 wt-% of total mixture) and [C_4vim][NTf_2] (0.55 g) were charged to a vial and dissolved with light heating in the dark using a vortex mixer. The monomer solution was then dispensed by syringe between two Rain-X® treated glass slides, separated by a 0.5 mm PTFE spacer, held together by binder clips. The apparatus was exposed to a broadband UV lamp (UVP

Blak-Ray™ B-100AP High-Intensity UV Lamp) for 5 min on each side. The resulting semi-IPNs were kept in a vacuum oven (60 °C, < 0.1 mm Hg) for 48 h prior to analysis.

Materials Characterization: The structure and functionality of the AC API monomer and each ionene were confirmed using ^{1}H-NMR spectroscopy (**Figures S1-S4**). The number average molecular weights (M_n) for these ionenes were calculated via end group analysis utilizing ^{1}H NMR spectroscopy. The residual monomer end groups are identifiable C(2,4,5)-H peaks of the imidazole rings, which experience a downfield shift when converted to the imidazolium form upon polymerization. Glass transition temperatures (T_g) of the AC API ionenes and semi-IPNs were evaluated using a TA Instruments Q200 differential scanning calorimeter (DSC) at a heating rate of 2°C/min on 4-8 mg samples under a dry N_2 atmosphere (error of $\pm$ 2.0 °C from duplicate runs). The T_g values were determined from the inflection point for each network from the second heating event. Thermal stability ($T_{d5\%}$) studies were completed in duplicate on each sample using a TA Instruments Q500 thermogravimetric analyzer (TGA) under a constant dry nitrogen flow at a heating rate of 10°C/min. $T_{d5\%}$ is defined as temperature at which 5% weight loss of the polymer sample was observed. A TA Instruments Q800 DMA with a single frequency of 1 Hz at a heating rate of 5 °C/min in film tension mode was utilized to determine mechanical properties. DMA experiments were completed in duplicate on each sample. Tensile testing was conducted by cutting rectangular strips of each polymer samples and securing each one with the DMA film clamps. The extension was increased at a rate of 20 mm/min at 25 ºC, with a preload force of 0.01 N, until each sample broke or the measurements exceeded the capabilities of the instrument. Each semi-IPN was tested in triplicate, and average stress and strain at break measurements are reported.

Conductivity Experiments: Anhydrous ionic conductivities were measured using a TA Instruments DHR-2 Discovery Hybrid Rheometer with dielectric accessory and Keysight

Technologies E4980AL/120 LCR meter was utilized. Each sample was first dried in a vacuum oven for 48 h (60 °C, < 0.01 mm Hg). To determine their anhydrous nature, each sample was analyzed isothermally by TGA after drying (2 hours at 150 ˚C). Results from these experiments indicated weight loss of less than 0.05% across all specimens. Then, the sample with approximate thickness of 500 μm was placed between the two 25 mm stainless steel, parallel plate electrodes of the dielectric accessory and the environmental chamber, under an atmosphere of dry nitrogen and cooled with liquid nitrogen, was closed. Dielectric permittivity and conductivity were measured isothermally with an ac amplitude of ± 0.01 V in 10 °C steps over a frequency range of 20.0-10^6 Hz. Samples were kept at a constant axial force of 5.0 ± 0.2 N and allowed to soak at each temperature for 45 minutes prior to obtaining measurements. The DC-conductivity (σ_{DC}) was determined from the plateau value observed in the spectral dependence of the conductivity function ($\sigma' = \omega\varepsilon''\varepsilon_o$ where ω is the frequency, ε'' is the dielectric loss and ε_o is the vacuum permittivity).

RESULTS AND DISCUSSION

Preparation and Characterization of the AC API ionenes and semi-IPNs. These polyamide-ionenes, which share common structural elements with Nylon-6®, were prepared from AC API by reacting an excess of API with AC under interfacial reaction conditions (**Scheme 1**). The polyamide-ionenes of interest were prepared using a two-step process. First, the AC API monomer was coupled with the appropriate dihalide: DiBr-HEX, DiBr-DEC, or *p*DCX. The second step involved taking the crude reaction solution and pouring it onto a solution of $LiNTf_2$ in DI water with vigorous mechanical mixing. This promoted the desired anion metathesis evidenced by the induced hydrophobicity (the ionenes as the halide salts are fully water soluble) and precipitation which allowed for isolation of the AC API [NTf_2] ionenes, which were subsequently purified, resulting in a series of viscous oils.

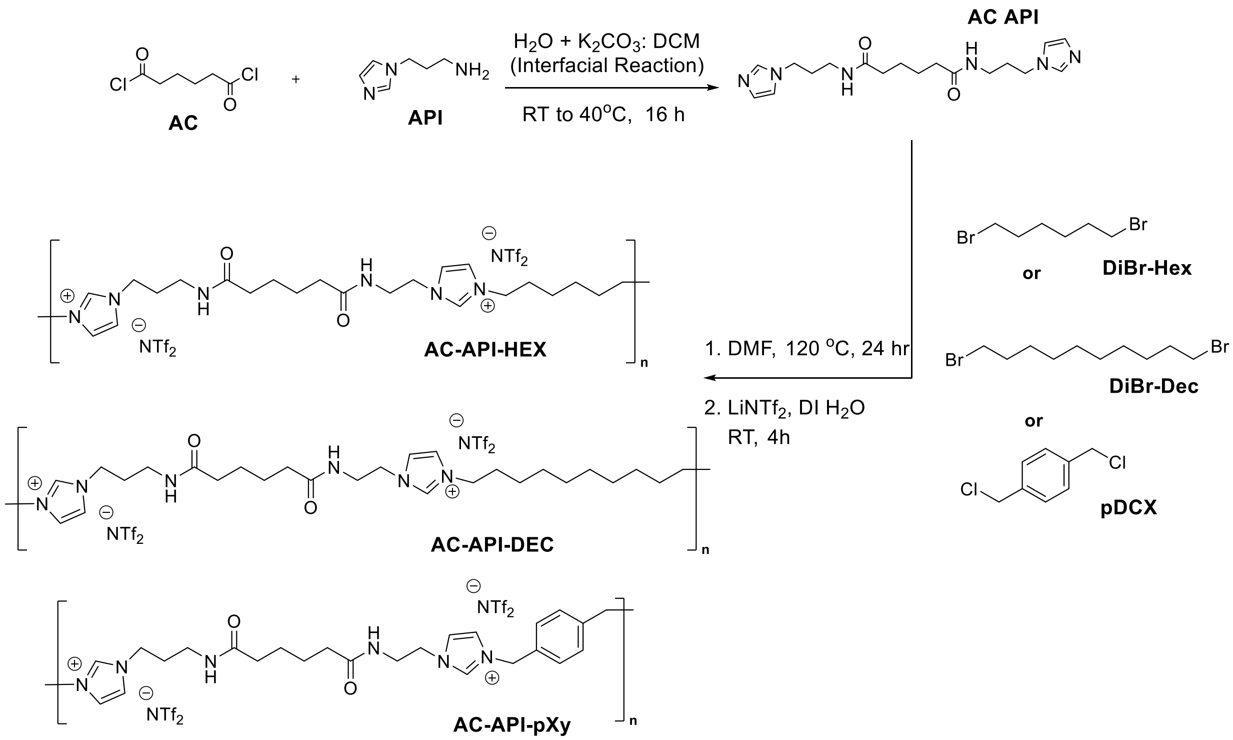

Scheme 1: Synthesis of AC API imidazolium-based ionenes.

The polyamide-ionenes were characterized by ^{1}H NMR spectroscopy (**Figures S2-S4**). M_n values, calculated from end-group analysis, were 100 kDa (AC-API-HEX), 86 kDa (AC-API-DEC), and 70 kDa (AC-API-pXy). Polymerizations via the Menshutkin reaction proceed as a step growth process; thus, the Carothers' equation was employed to approximate a corresponding number average degree of polymerization, $X_n \approx 67$-100 ($\rho \approx 0.985$-0.990). Thermal analysis of the ionenes were completed using DSC and TGA (**Table 1**). Each AC API ionene exhibited a glass transition (T_g) value, with AC-API-DEC exhibiting the lowest T_g at -32.4 °C (**Figure S5**). Higher T_g values were observed for AC-API-HEX, which had a shorter alkyl spacer length and AC-API-pXy which is a more compact and rigid aromatic linker. Of additional note were several smaller transitions in the DSC thermogram of AC-API-DEC above the T_g, which are indicative of possible mesogenic behavior. As the alkyl spacer between imidazolium groups grows from hexyl to decyl, there is the increased potential for chain alignment and long-range order (presumably via amide H-bonding). Similar behavior was previously described for a series of liquid crystalline polyesters by Lenz,[65] and has also been observed for PILs with longer alkyl side chains and other ionenes with long alkyl spacer lengths.[15,17] Thermal stabilities ($T_{d5\%}$ values) of the AC-API ionenes were found to be between 240-310 °C (**Figure S6**).

Table 1. Molecular Weights and Thermal Properties of AC API ionenes.

Network	^{1}H NMR M_n (kDa)	DSC T_g (°C)	TGA $T_{d5\%}$ (°C)
AC-API-HEX	100	-27.9	306
AC-API-DEC	86	-32.4	241
AC-API-pXy	70	5.7	292

Semi-IPNs were then prepared by first dissolving the appropriate AC API ionene (10 or 20 wt-%) in [C_4VIm][NTf_2] monomer. The crosslinker, trimethyloylpropane ethoxylate triacrylate (ETMPTA, M_n ~ 428) was then added (10 wt-%), followed by addition and dissolution of the photoinitiator TPO (diphenyl(2,4,6-trimethylbenzoyl)phosphine oxide) (1 wt-% based upon alkene). The resulting homogenous mixture was then dispensed by syringe between two Rain-X® treated glass slides, separated by a 500 μm Teflon spacer. The apparatus was placed under a broadband UV lamp to induce photopolymerization (**Scheme 2**). The resulting films were removed and dried in a vacuum oven (60 °C, < 0.01 mm Hg) for 48 h prior to any analysis. Any attempts to increase the ionene content above 20 wt% led to separation of the ionene during polymerization. The semi-IPNs prepared using 10-20 wt% of the ionene were found to be stable with no evidence of ionene separation after storage for several months in a desiccator.

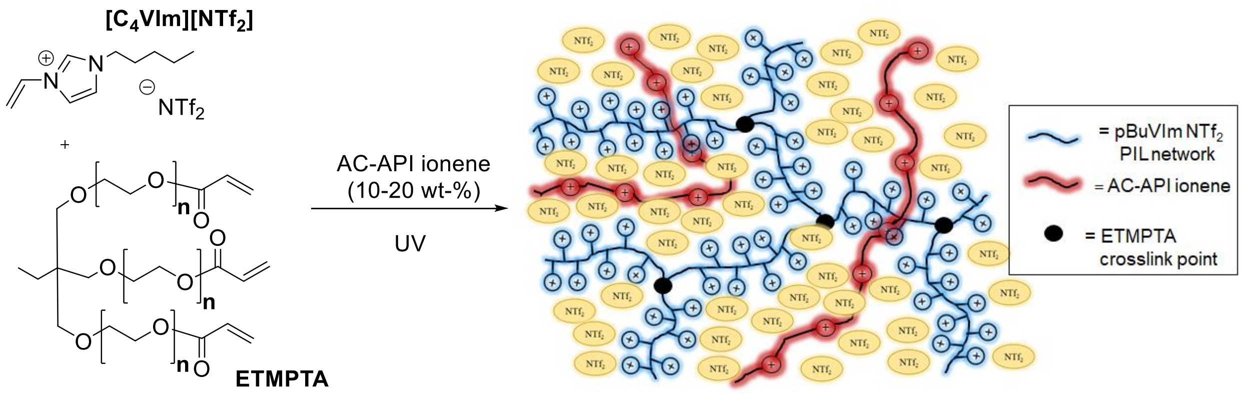

Scheme 2: Synthesis of semi-interpenetrating networks.

The resulting semi-IPNs were initially analyzed by DSC for their thermal properties in order to identify any thermal transitions. Inclusion of the ionene, at any concentration, led to a relatively weak secondary phase transition, identified as the T_g (**Figures S7-S9**). The observation of a single T_g is indicative of a well-mixed blend of the ionene and the PIL network in the semi-IPN; however, the broadness of the temperature interval in which the T_g occurs may indicate some degree of nanoscale heterogeneity. The T_g values for all of the semi-IPNs were below that of the model PIL network as the ionene is expected to act in part as a plasticizer (**Table 2**). While gradual addition of 10- and 20-wt% AC-API-HEX to the poly([C_4VIm][NTf_2]) PIL network resulted in the corresponding lowering of the T_g to -2.3 and -18.9 °C, respectively, analogous additions of AC-API-DEC and AC-API-pXy resulted in an initial drop in T_g with 10-wt% addition, but then an increase when 20-wt% was used. We hypothesize that the longer C10 linker for AC-API-DEC may participate in some long-range ordering (as noted in the discussion of the DSC thermogram for the pure ionene). A similar argument could be made with regards to the π-π interactions between aryl rings of AC-API-pXy. However, it is also possible in both cases that, by including a larger concentration of non-ionic side chains into the semi-IPN that some degree of nanophase separation could be occurring, causing ionic groups to become clustered or aggregated. This would result in an increase in ionic interactions and could lead to an increase in T_g. Thermogravimetric analysis (TGA) was utilized to determine the thermal stabilities of the semi-IPNs (**Figure S10-S12**). While the AC-API ionenes all exhibited $T_{d5\%}$ values < 310 °C, the poly([C_4VIm][NTf_2]) PIL network showed thermal stability up to ~335 °C. The semi-IPNs were found to display $T_{d5\%}$ values that more closely resembled the PIL network (> 320 °C across all samples), which makes sense as the ionene only accounts for 10-20 wt-% in the overall material.

Table 2. Thermal Properties of the semi-IPNs.

Network	DSC T_g (°C)	TGA $T_{d5\%}$ (°C)	Network	DSC T_g (°C)	TGA $T_{d5\%}$ (°C)
p[C_4VIm][NTf_2]	32.7	338	sIPN-DEC-10	-19.2	330
sIPN-HEX-10	-2.3	342	sIPN-DEC-20	7.6	333
sIPN-HEX-20	-18.9	321	sIPN-pXy-10	8.9	334
			sIPN-pXy-20	12.8	337

Mechanical properties of the networks. The semi-IPNs were next analyzed for their mechanical properties by DMA. Crosslink density (ρ_x) was calculated from the rubbery plateau value (E' at 120 °C) of each semi-IPN according to rubbery elasticity theory using the following equation: $\rho_x = E'/3RT$ (**Table 3**).[43,44] As expected, inclusion of the non-covalently bound ionene effectively dilutes the number of crosslinks in the bulk sample, leading to lower ρ_x values. This result is reflected in an even lower crosslink density when the ionene content was increased from 10- to 20-wt%. Still, the rubbery plateau values of all of the semi-IPNs were in excess of 1.0 MPa and linear above their respective T_g values (**Figure 1**). Inclusion of the AC-API-HEX ionene had the largest effect on the rubbery plateau modulus. Trends in the DMA T_g values, determined from the tan delta maxima, were analogous to that of the DSC T_g results previously described. Similar to their DSC thermograms, tan delta curves for sIPN-HEX-20 and sIPN-DEC-20 were found to be rather broad, indicating some degree of heterogeneity in these samples (**Figures S13-S14**).

Table 3. Mechanical Properties of the semi-IPNs.

Network	E' @ 120 °C (MPa)	tan δ max (°C)	ρ_x x 10^{-4} (mol/cm^3)	Stress at break (MPa)	Strain at break (%)
p[C_4VIm][NTf_2]	2.47 ± 0.15	72.3 ± 0.4	2.52 ± 0.1	N/A	N/A
sIPN-HEX-10	2.33 ± 0.14	39.7 ± 0.4	2.38 ± 0.3	0.82 ± 0.06	37.0 ± 5.0
sIPN-HEX-20	1.02 ± 0.12	33.9 ± 0.5	0.95 ± 0.1	0.27 ± 0.05	17.9 ± 1.0
sIPN-DEC-10	1.71 ± 0.16	62.3 ± 0.5	1.74 ± 0.1	2.46 ± 0.32	37.6 ± 5.0
sIPN-DEC-20	1.67 ± 0.13	48.3 ± 0.4	1.97 ± 0.1	0.73 ± 0.05	27.9 ± 2.3
sIPN-pXy-10	1.70 ± 0.12	55.7 ± 0.4	1.73 ± 0.1	1.32 ± 0.11	54.1 ± 7.4
sIPN-pXy-20	1.55 ± 0.15	59.1 ± 0.5	1.58 ± 0.1	2.51 ± 0.08	75.8 ± 7.5

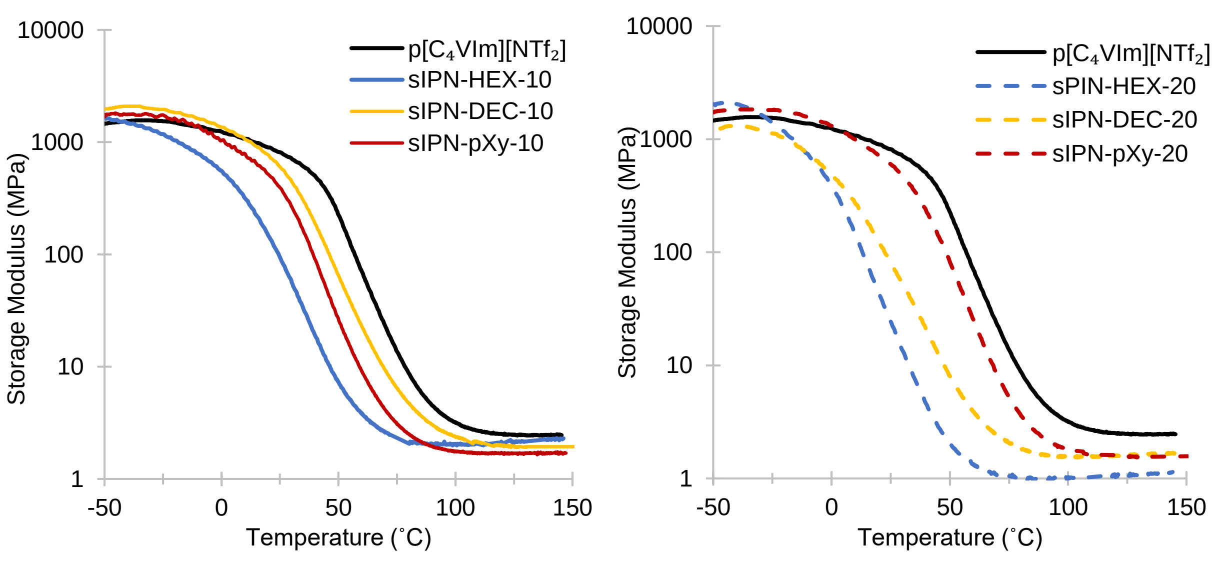

Figure 1: Storage modulus (E') curves for the semi-IPNs at 10-wt% AC-API ionene (left) and 20-wt% ionene (right). For reference, the storage modulus curve for the p[C_4VIm][NTf_2] PIL network in included on each graph.

Stress-strain data was obtained using DMA in tensile mode. The p[C_4VIm][NTf_2] PIL network was very stiff and the stress and strain at break could not be measured as the values surpassed the capabilities of the instrument. Inclusion of the AC-API ionenes with alkyl spacers led to a dramatic drop in the mechanical stability of the material; however, increased flexibility was observed. Representative curves for each semi-IPN are shown in **Figure 2** with stress and strain at break values reported in **Table 3**. Triplicate runs for each semi-IPN can be found in the Supporting Information (**Figures S15-S20**). The sIPN-HEX systems were the least mechanically stable of all of the materials studied in terms of stress at break, nor did these systems provide much of an advantage in terms of elongation at break. Substitution with the AC-API-DEC ionene boosted the stress and strain at break of the resulting semi-IPNs compared to the AC-API HEX analogs; however, increasing the AC-API-DEC content from 10- to 20-wt% decreased the mechanical strength with similar elongation at break. The largest stress (and strain) at break for each series (10- and 20-wt%) was observed for the sIPN-pXy systems. The inclusion of the rigid aromatic moieties must provide some mechanical stability to the ionene and thus to the semi-IPN. Furthermore, the ionene itself must have a better ability to flow within the semi-IPN as the material is being extended, leading to a larger elongation at break. It is worth noting that, in both the 10- and 20-wt% AC-API-pXy systems that some yielding of the material was observed at approximately 20-25% strain. Overall, the semi-IPNs were found to exhibit slightly higher stress and strain at break values when compared with other IPNs which were composed of a pyrrolidinium-containing PIL network and an epoxy-amine, polybutadiene or nitrile butadiene rubber non-ionic polymer.[59,60]

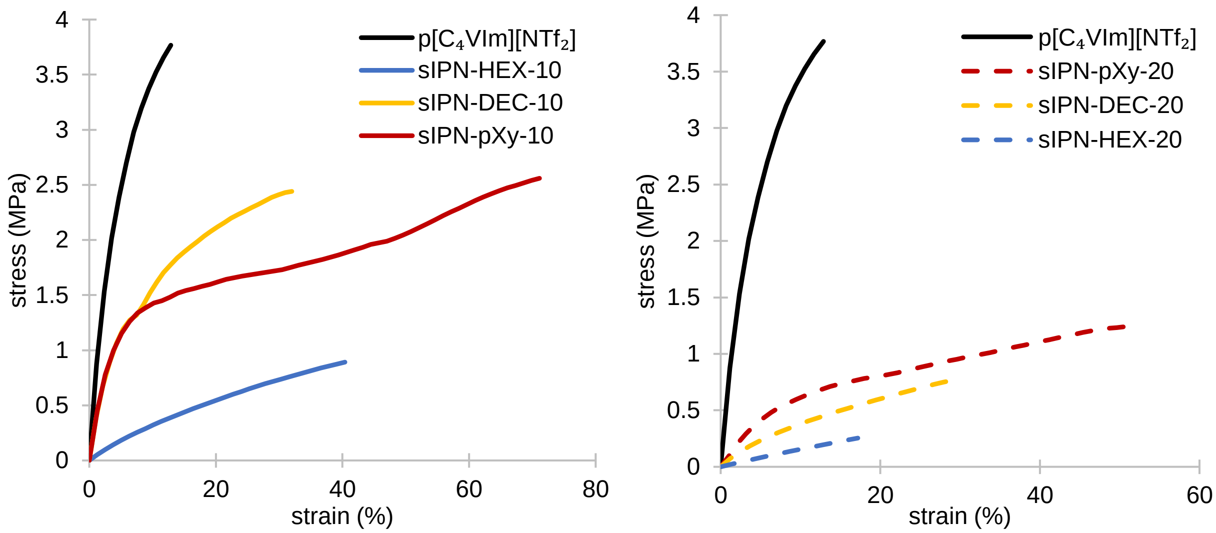

Figure 2: Representative DMA stress-strain curves for semi-IPNs containing 10-wt% AC-API ionene (left) and 20-wt% AC-API ionene (right).

Anhydrous ionic conductivities were determined for each semi-IPN as well as the model p[C_4Vim][NTf_2] PIL network using the dielectric spectroscopy accessory of a rheometer. Regardless of which ionene or at what wt% the ionene was added, all of the semi-IPNs exhibited higher ionic conductivities (10^{-5} to 10^{-7} S/cm at 30 °C) compared to the pBuVIM NTf_2 PIL network (1.70 x 10^{-8} S/cm at 30 °C). In addition, for each ionene semi-IPN type (HEX, DEC, pXy), an increase in ionene content from 10- to 20-wt% led to an enhancement in conductivity of one to two orders of magnitude at 30 °C. As all of the data collected was near to or above the T_g value of the respective semi-IPN, each ionic conductivity curve was fitted to the Vogel-Fulcher-Tamman (VFT) equation:

$$\sigma(T) = \sigma_\infty \times \exp\left(\frac{-DT_o}{T - T_o}\right)$$

where σ_∞ is the infinite temperature conductivity limit, T_o is the Vogel temperature (where ionic conductivity diverges to zero) and D is the strength parameter, which is inversely related to dynamic fragility.[29,33,44] Theoretical log σ values generated from the VFT fittings are represented as solid lines in **Figure 3** and the VFT parameters are provided in **Table 4**. The high temperature conductivity (σ_∞) increased three- to six-fold when 10-wt% of an ionene was added to the PIL network, with a further rise observed when the amount was increased to 20-wt%. This suggests that inclusion of the ionene helps to facilitate ion transport. This could be due to the ionene forcing larger free volume/mesh sizes in the network structure as it has been suggested that the transport of larger, less Lewis basic anions like [NTf_2] depend strongly on elastic energy barriers.[66] It is also possible that inclusion of the ionene allows for better solvation of ion pairs. At 10-wt% ionene, AC-API-pXy appears to be the most effective at enhancing ion transport with a σ_∞ value of 10.4 S/cm; however, a large jump in σ_∞ was noted when the amount of AC-API-DEC was increased from 10- to 20-wt% (4.8 S/cm to 16.5 S/cm, respectively). This increase in σ_∞ could be due to phase separation effects, where ion channels or percolated aggregates are being formed within the network due to the alignment of a larger concentration of non-ionic alkyl chains, facilitating ion transport.[36] Additional morphological studies or computational modeling would need to be done to help further elucidate the molecular structure of these semi-IPNs.

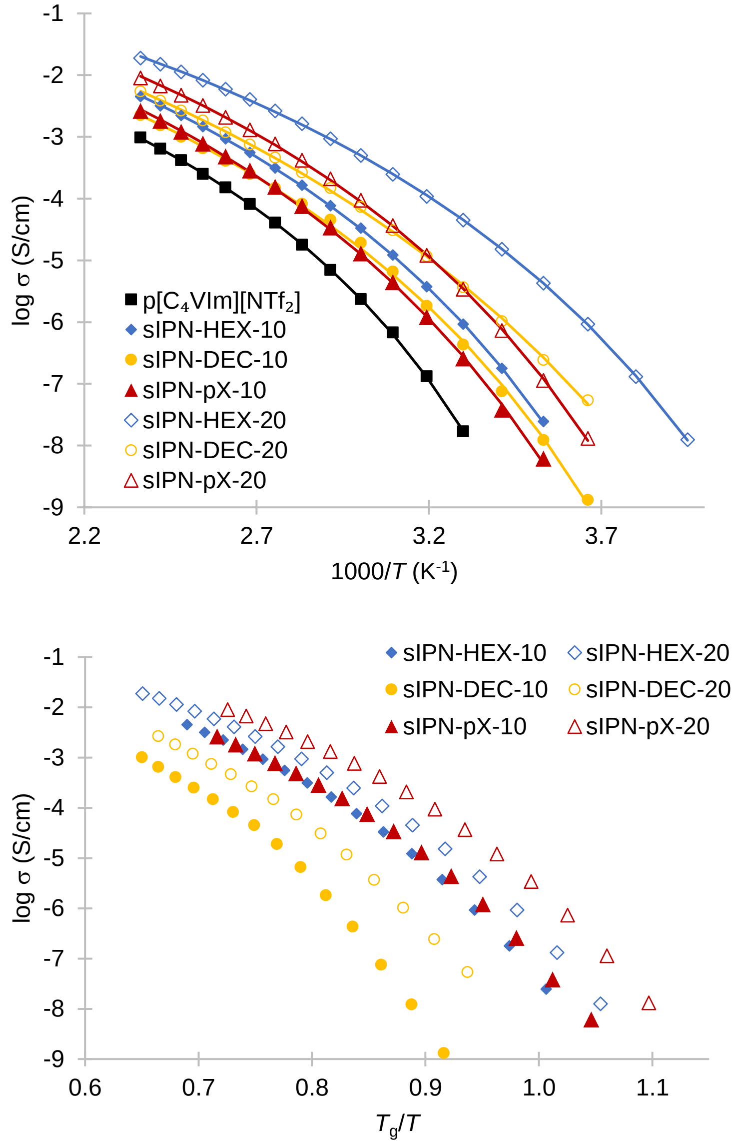

Figure 3. Anhydrous ionic conductivities of p[C_4Vim][NTf_2] PIL network and the semi-IPNs (top). T_g-normalized anhydrous conductivities for the semi-IPNs (bottom).

Table 4. VFT fitting parameters for the semi-IPNs.

Network	σ at 30 °C (S/cm)	σ_∞ (S/cm)	T_o (K)	T_g-T_o (K)	D
p[C_4VIm][NTf_2]	1.70 x 10^{-8}	1.55	221	85	6.5
sIPN-HEX-10	9.20 x 10^{-7}	8.33	197	74	8.6
sIPN-HEX-20	4.49 x 10^{-5}	12.10	177	77	8.9
sIPN-DEC-10	4.30 x 10^{-7}	4.78	194	60	9.1
sIPN-DEC-20	3.64 x 10^{-6}	16.45	170	90	11.9
sIPN-pXy-10	2.57 x 10^{-7}	10.44	196	86	9.6
sIPN-pXy-20	3.39 x 10^{-6}	13.77	193	93	8.7

The Vogel temperatures for the semi-IPNs were comparable or slightly higher (60-93 K) than values typically observed for previously reported IL-containing polymers and did not track directly with T_g.[33,43,44,67-69] As T_o and T_g are characteristic of divergence of ion conduction to zero and arrested segmental motion, respectively, and a larger difference between the two may indicate a greater decoupling between segmental dynamics and ionic conductivity.[33,68] The strength parameter (D) is inversely related to polymer dynamic fragility (m). While the p[C_4VIm][NTf_2] PIL network exhibited a D value comparable to other recently reported networks,[33,43,44] inclusion of the ionene lead to a significant increase in D, meaning that the materials exhibited lower fragilities. There does not appear to be a direct relationship between D and ionene structure or content at this point. What the data seems to indicate is that these semi-IPNs exhibit larger decoupling (high T_g-T_o values) and low fragility, which may reflect the influence of the linear ionene rather than the PIL network.[68] Furthermore, fragility does not appear to correlate in any reasonable fashion with T_g. As is evident from this data, the relationship between ionic conductivity and molecular structure is complex, even more so in semi-IPNs where there are two ion-containing polymers affecting ionic conductivity and further study is warranted to separate these interconnecting factors.

Conductivity was also normalized by plotting values against T_g/T to minimize the effect of T_g and segmental motion between semi-IPNs. The results are shown in **Figure 3**. While sIPN-HEX-10 and sIPN-pXy overlap reasonably well, the remaining curves do not appreciably coalesce, meaning that the changes in ionic conductivity are not solely due to polymer chain dynamics (i.e. not solely T_g dependent). This divergence becomes even larger as the temperature approaches the T_g. Moreover, the two sIPN-DEC systems were observed to have the lowest T_g-normalized conductivities (several orders of magnitude) at the lower temperatures. Overall, the semi-IPNs employing the AC-API-pXy ionene were observed to have the highest T_g-normalized ionic conductivity within each subset (10- and 20-wt%). It has been hypothesized that having a less flexible backbone may be beneficial to conductivity as temperature approaches the T_g;[37,72] however, it is also worth noting that the DEC systems contain the lowest wt% of ions relative to the HEX and pXy systems.

CONCLUSION

Ionic liquids and ionic polymers continue to provide a vast array of possibilities insofar as their structure-property relationships are concerned. As we continue to strive for improved performance in end-use applications, alternative approaches towards combining the properties of ILs and ionic polymers must be pursued. For the first time, poly(IL)-ionene semi-interpenetrating networks have been prepared by first dissolving the ionene in a vinyl-functionalized imidazolium IL, then photopolymerizing of the IL around the ionene. The polyamide-ionenes were prepared from amide-functionalized, bisimidazole monomers, coupled with various dihalide linkers bearing flexible (hexyl or decenyl) or rigid (*p*-xylyl) backbones. Addition of 10-20 wt% ionene to a covalently crosslinked p[C_4Vim][NTf_2] PIL network resulted in semi-IPNs which exhibited moderate to large reductions in DSC T_g compared to the PIL while maintaining thermal stability values in excess of 330 °C. DMA analysis of the semi-IPNs indicated rubbery plateau moduli in excess of 1.0 MPa with single (albeit sometimes broad) peaks in the tan delta signals, indicative of a homogenous material. Tensile testing indicated an increase in elasticity across all semi-IPNs as compared to the poly(ionic liquid).

All semi-IPNs exhibited higher ionic conductivities (10^{-5} to 10^{-7} S/cm at 30 °C) compared to the p[C_4Vim][NTf_2] PIL with increased conductivity observed (one to two orders of magnitude) when the ionene content was increased from 10- to 20-wt%. VFT fitting of the conductivity curves indicated that high temperature conductivities (σ_∞) increased three- to six-fold when 10-wt% of an ionene (with a further increase at 20-wt%) which is indicative of enhanced ion transport upon inclusion of the ionene. Relatively large differences between T_o and T_g may indicate a greater decoupling between segmental dynamics and ionic conductivity, with a larger difference observed with higher ionene content. T_g-normalization of the data indicated that changes in ionic conductivity are not solely due to T_g (polymer chain dynamics). As there are two ion-containing polymers affecting conductivity in these semi-IPNs, the relationship between molecular structure, morphology and conductivity properties is complex and further study is necessary to understand these interrelated factors while fine tuning their overall properties.

ASSOCIATED CONTENT

The Supporting Information is available free of charge and includes relevant 1H NMR spectra, DSC and TGA curves for monomers and semi-IPNs as well as DMA tan delta and stress-strain curves for semi-IPNs.

ACKNOWLEDGEMENTS

Support for this work provided by the United States Department of Energy Office of Science (DE-SC0020282) through the Separations and EPSCoR programs and Energy Efficiency and Renewable Energy Advanced Manufacturing Office is gratefully acknowledged. JEB acknowledges partial support from the NSF (CBET-1605411) while KEO acknowledges a GAANN Fellowship from the United States Department of Education (P200A180056). KMM and GMT acknowledge partial support from the NSF (DMR-1708632 and DMR-1828251). KMM would also like to acknowledge Dr. R. Daniel Johnson for helpful discussions regarding the analysis of the ionic conductivity data.

ORCID Information for Authors:

Kathryn E. O’Harra: 0000-0001-5328-0024

Jason E. Bara: 0000-0002-8351-2145

Kevin M. Miller: 0000-0001-5314-7477

REFERENCES

1. Shaplov, A. S.; Marcilla, R.; Mecerreyes, D. Recent advances in innovative polymer electrolytes based on poly(ionic liquid)s. *Electrochim. Acta* **2015,** *175*, 18-34.

2. Zhao, J.; Lei, Q.; He, F.; Zheng, C.; Liu, Y.; Zhao, X.; Yin, J. Interfacial polarization and electroresponsive electrorheological effect of anionic and cationic poly(ionic liquid)s. *ACS Appl. Polym. Mater.* **2019,** *1(11)*, 2862-2874.

3. Lodge, T. P.; Ueki, T. Mechanically tunable, readily processable ion gels by self-assembly of block copolymers in ionic liquids. *Acc. Chem. Res.* **2016,** *49*, 2107-2114.

4. Margaretta, E.; Fahs, G. B.; Inglefield, D. L.; Jangu, C.; Wang, D.; Heflin, J. R.; Moore, R. B.; Long, T. E. Imdazolium-containing ABA triblock copolymers as electroactive devices. *ACS Appl. Mater. Interfaces* **2016,** *8*, 1280-1288.

5. Osada, I.; de Vries, H.; Scrosati, B.; Passerini, S. Ionic-liquid-based polymer electrolytes for battery applications. *Angew. Chem. Int. Ed.* **2016,** *55*, 500-513.

6. Robertson, N. J.; Kostalik IV, H. A.; Clark, T. J.; Mutolo, P. F.; Abruña, H. D.; Coates, G. W. Tunable high performance cross-linked alkaline anion exchange membranes. *J. Am. Chem. Soc.* **2010,** *132*, 3400-3404.

7. Lin, B.; Qiu, L.; Qiu, B.; Peng, Y.; Yan, F. A soluble and conductive polyfluorene ionomer with pendant imidazolium groups for alkaline fuel cell applications. *Macromolecules* **2011,** *44*, 9642-9649.

8. O'Harra, K. E.; Kammakakam, I.; Noll, D. M.; Turfinger, E. M.; Dennis, G. P.; Jackson, E. M.; Bara, J.E. Synthesis and performance of aromatic polyamide ionenes as gas separation membranes. *Membranes* **2020,** *10*, 51-66.

9. Mittenthal, M.S.; Flowers, B.S.; Bara, J.E.; Whitley, J.W.; Spear, S.K.; Roveda, J. D.; Wallace, D.A.; Shannon, M.S.; Holler, R.; Martens, R.; Daly, D.T. Ionic polyimides: hybrid polymer architectures and composites with ionic liquids for advanced gas separation membranes. *Ind. Eng. Chem. Res.* **2017,** *56*, 5055.

10. Zulfigar, S.; Sarwar, M.I.; Mecerreyes, D. Polymeric ionic liquids for CO_2 capture and separation: potential, progress and challenges. *Polym. Chem.* **2015,** *6*, 6435-6451.

11. Cowan, M.G.; Gin, D. L.; Noble, R. D. Poly(ionic liquid)/ionic liquid ion-gels with high "free" ionic liquid content: platform materials for CO_2/light gas separations. *Acc. Chem. Res.* **2016,** *49*, 724-732.

12. Muñoz-Bonilla, A.; Fernández-García, M. Poly(ionic liquid)s as antimicrobial materials. *Eur. Polym. J.* **2018,** *105*, 135-149.

13. Yuan, J.; Mecerreyes, D.; Antonietti, M. Poly(ionic liquid)s: an update. *Prog. Polym. Sci.* **2013,** *38(7)*, 1009-1036.

14. Qian, W.; Texter, J.; Yan, F. Frontiers in poly(ionic liquid)s: syntheses and applications. *Chem. Soc. Rev.* **2017,** *46(4)*, 1124-1159.

15. Yuan, J.; Antonietti, M. Poly(ionic liquid)s: Polymers expanding classical property profiles. *Polymer* **2011,** *52(7)*, 1469-1482.

16. Williams, S. R.; Long, T. E. Recent advances in the synthesis and structure-property relationships of ammonium ionenes. *Prog. Polym. Sci.* **2009,** *34*, 762-782.

17. Bara, J. E.; O'Harra, K. E. Recent advances in the design of ionenes: Toward convergence with high-performance polymers. *Macromol. Chem. Phys.* **2019,** *220(13)*, 1900078.

18. O'Harra, K. E.; Bara, J. E. Toward controlled functional sequencing and hierarchical structuring in imidazolium ionenes. *Polym. Int.* **2020,** *in press*. https://doi.org/10.1002/pi.6109

19. Choi, U. H.; Lee, M.; Wang, S.; Liu, W.; Winey, K. I.; Gibson, H. W.; Colby, R. H. Ionic conduction and dielectric response of poly(imidazolium acrylate) ionomers. *Macromolecules* **2012,** *45*, 3974-3985.

20. Whitely, J. W.; Horne, W. J.; Shannon, M. S.; Andrews. M. A.; Terrell, K. L.; Hayward, S. S.; Yue, S.; Mittenthal, M. S.; O'Harra, K. E.; Bara, J. E. Systematic investigation of the photopolymerization of imidazolium-based ionic liquid styrene and vinyl monomers. *J. Polym. Sci. A Polym. Chem.* **2018,** *56*, 2364-2375.

21. Ohno, H. Molten salt type polymer electrolytes. *Electrochim. Acta* **2001,** *46*, 1407-1411.

22. Washiro, S.; Yoshizawa, M.; Nakajima, H.; Ohno, H. Highly ion conductive flexible films composed of network polymers based on polymerizable ionic liquids. *Polymer* **2004,** *45*, 1577-1582.

23. Nakajima, H.; Ohno, H. Preparation of thermally stable polymer electrolytes from imidazolium-type ionic liquid derivatives. *Polymer* **2005,** *46*, 11499-11504.

24. Green, M. D.; Salas-de la Cruz, D.; Ye, Y.; Layman, J. M.; Elabd, Y. A.; Winey, K. I.; Long, T. E. Alkyl-substituted *N*-vinylimidazolium polymerized ionic liquids: Thermal properties and ionic conductivities. *Macromol. Chem. Phys.* **2011,** *212*, 2522-2528.

25. Salas-de la Cruz, D.; Green, M. D.; Ye, Y.; Elabd, Y. A.; Long, T. E.; Winey, K. I. Correlating backbone-to-backbone distance to ionic conductivity in amorphous polymerized ionic liquids. *J. Polym. Sci. B. Polym. Phys.* **2012,** *50*, 338-346.

26. Lee, M.; Choi, U. H.; Colby, R. H.; Gibson, H. W. Ion conduction in imidazolium acrylate ionic liquids and their polymers. *Chem. Mater.* **2010,** *22*, 5814-5822.

27. Fan, F.; Wang, Y.; Hong, T.; Heres, M. F.; Saito, T.; Sokolov, A. P. Ion conduction in polymerized ionic liquids with different pendant groups. *Macromolecules* **2015,** *48*, 4461-4470.

28. Choi, J.-H.; Ye, Y.; Elabd, Y. A.; Winey, K. I. Network structure and strong microphase separation for high ion conductivity in polymerized ionic liquid block copolymers. *Macromolecules* **2013,** *46*¸5290-5300.

29. Jangu, C.; Wang, J. H.; Wang, D.; Sharick, S.; Heflin, J. R.; Winey, K. I.; Colby, R. H.; Long, T. E. Well-defined imidazolium ABA triblock copolymers as ionic-liquid-containing electroactive membranes. *Macromol. Chem. Phys.* **2014,** *215*¸1319-1331.

30. Meek, K. M.; Elabd, Y. A. Polymerized ionic liquid block copolymers for electrochemical energy. *J. Mater. Chem. A* **2015,** *3*, 24187-24194.

31. Meek, K. M.; Sharick, S.; Ye, Y.; Winey, K. I.; Elabd, Y. A. Bromide and hydroxide conductivity-morphology relationships in polymerized ionic liquid block copolymers. *Macromolecules* **2015,** *48*¸4850-4862.

32. Tamami, M.; Salas-de la Cruz, D.; Winey, K. I.; Long, T. E. Structure-property relationships of water-soluble ammonium-ionene copolymers. *Macromol. Chem. Phys.* **2012,** *213*, 965-972.

33. Zhao, Q.; Shen, C.; Halloran, K. P.; Evans, C. M. Effect of network architecture and linker polarity on ion aggregation and conductivity in precise polymerized ionic liquids. *ACS Macro Lett.* **2019,** *8*, 658-663.

34. Hemp, S. T.; Zhang, M.; Tamami, M.; Long, T. E. Phosphonium ionenes from well-defined step-growth polymerization: thermal and melt rheological properties. *Polym. Chem.* **2013,** *4*, 3582-3590.

35. Williams, S. R.; Salas-de la Cruz, D.; Winey, K. I.; Long, T. E. Ionene segmented block copolymers containing imidazolium cations: Structure-property relationships as a function of hard segment content. *Polymer* **2010,** *51*, 1252-1257.

36. O'Harra, K. E.; Kammakakam, I.; Bara, J. E.; Jackson, E. M. Understanding the effects of backbone chemistry and anion type on the structure and thermal behaviors of imidazolium polyimide-ionenes. *Polym. Int.* **2019,** *68*, 1547-1556.

37. Schreiner, C.; Bridge, A. T.; Hunley, M. T.; Long, T. R.; Green, M. D. Segmented imidazolium ionenes: solution rheology, thermomechanical properties, and electrospinning. *Polymer* **2017,** *114*, 257-265.

38. O'Harra, K. E.; Noll, D. M.; Kammakakam, I.; DeVriese, E. M.; Solis, G.; Jackson, E. M.; Bara, J. E. Designing imidazolium poly(amide-amide) and poly(amide-imide) ionenes and their interactions with mono- and tri(imidazolium) ionic liquids. *Polymers* **2020,** *12*, 1254.

39. Morozova, S. M.; Shaplov, A. S.; Lozinskaya, E. I.; Mecerreyes, D.; Sardon, H.; Zulfiqar, S.; Suarez-Garcia, F.; Vygodskii, Y. S. Ionic polyurethanes as a new family of poly(ionic liquid)s for efficient CO_2 capture. *Macromolecules* **2017,** *50*, 2814-2824.

40. Gao, R; Zhang, M.; Wang, S.; Moore, R. B.; Colby, R. H.; Long, T. E. Polyurethanes containing an imidazolium diol-based ionic-liquid chain extender for incorporation of ionic-liquid electrolytes. *Macromol. Chem. Phys.* **2013,** *214*, 1027-1036.

41. Lee, M.; Choi, U. H.; Salas-de la Cruz, D.; Mittal, A.; Winey, K. I.; Colby, R. H.; Gibson, H. W. Imidazolium polyesters: structure-property relationships in thermal behavior, ionic conductivity, and morphology. *Adv. Funct. Mater.* **2011,** *21*, 708-717.

42. Kim. S.; Miller, K. M. Synthesis and thermal analysis of crosslinked imidazolium-containing polyester networks prepared by Michael addition polymerization. *Polymer* **2012,** *53*, 5666-5674.

43. Tracy, C. A.; Adler, A. M.; Nguyen, A.; Johnson, R. D.; Miller, K. M. Covalently crosslinked 1,2,3-triazolium-containing polyester networks: Thermal, mechanical and conductive properties. *ACS Omega* **2018,** *3*, 13442-13453.

44. Rhoades, T. C.; Wistrom, J. C.; Johnson, R. D.; Miller, K. M. Thermal, mechanical and conductive properties of imidazolium-containing thiol-ene poly(ionic liquid) networks. *Polymer* **2016,** *100*, 1-9

45. Bratton, A. F.; Kim, S.; Ellison, C. J.; Miller, K. M. Thermomechanical and conductive properties of thiol-ene poly(ionic liquid) networks containing backbone and pendant imidazolium groups. *Ind. Eng. Chem. Res.* **2018,** *57*, 16526-16536.

46. Zhao, J.; Lei, Q.; He, F.; Zheng, C.; Liu, Y.; Zhao, X.; Yin, J. Interfacial polarization and electroresponsive electrorheological effect of anionic and cationic poly(ionic liquid)s. *ACS Appl. Polym. Mater.* **2019,** *1*, 2862-2874.

47. Iacob, C.; Matsumoto, A.; Brennan, M.; Liu, H.; Paddison, S. J.; Urakawa, O.; Inoue, T.; Sangoro, J.; Runt, J. Polymerized ionic liquids: Correlation of ionic conductivity with nanoscale morphology and counterion volume. *ACS Macro Lett.* **2017,** *6*, 941-946.

48. Keith, J. R.; Rebello, N. J.; Cowen, B. J.; Ganesan, V. Influence of counterion structure on conductivity of polymerized ionic liquids. *ACS Macro Lett.* **2019,** *8*, 387-392.

49. Choi, U. H.; Ye, Y.; Salas-de la Cruz, D.; Liu, W.; Winey, K. I.; Elabd, Y. A.; Runt, J.; Colby, R. H. Dielectric and viscoelastic responses of imidazolium-based ionomers with different counterions and side chain lengths. *Macromolecules* **2014,** *47*, 777-790.

50. Delhorbe, V.; Bresser, D.; Mendil-Jakani, H.; Rannou, P.; Bernard, L.; Gutel, T.; Lyonnard, S.; Picard, L. Unveiling the ion conduction mechanism in imidazolium-based poly(ionic liquids): A comprehensive investigation of the structure-to-transport interplay. *Macromolecules* **2017,** *50*, 4309-4321.

51. Evans, C. M.; Bridges, C. R.; Sanoja, G. E.; Bartels, J.; Segalman, R. A. Role of Tethered Ion Placement on Polymerized Ionic Liquid Structure and Conductivity: Pendant versus Backbone Charge Placement. *ACS Macro Lett.* **2016,** *5*, 925-930.

52. Sterling, L. H., Klemper, D.; Utracki, L. A., eds. *Interpenetrating Polymers Networks*, **1991,** American Chemical Society: Washington, D. C.

53. IUPAC. Compendium of Chemical Terminology, 2nd ed. (the "Gold Book"). Compiled by A. D. McNaught and A. Wilkinson. Blackwell Scientific Publications, Oxford (1997).

54. Vidal, F.; Juger, J.; Chevrot, C.; Teyssié, D. Interpenetrating polymer networks from polymeric imidazolium-type ionic liquid and polybutadiene. *Polym. Bull.* **2006,** *57*, 473-480.

55. Becht, G. A.; Sofos, M.; Seifert, S.; Firestone, M. A. Formation of a liquid-crystalline interpenetrating poly(ionic liquid) network hydrogel. *Macromolecules* **2011,** *44*, 1421-1428.

56. Zhang, C.; Zhang, W.; Gao, H.; Bai, Y.; Sun, Y.; Chen, Y. Synthesis and gas transport properties of poly(ionic liquid) based semi-interpenetrating polymer network membranes for CO_2/N_2 separation. *J. Membr. Sci.* **2017,** *528*,72-81.

57. Tudor, A.; Florea, L.; Gallagher, S.; Burns, J.; Diamond, D. Poly(ionic liquid) semi-interpenetrating network multi-responsive hydrogels. *Sensors* **2016,***16*, 219.

58. Kanaan, A. F.; Barsan, M. M.; Brett, C. M. A.; Alvarez-Lorenzo, C.; Cocheiro, A.; de Sousa, H. C.; Dia, A. M. A. Sustainable electro-responsive semi-interpenetrating starch/ionic liquid copolymer networks for the controlled sorption/release of biomolecules. *ACS Sustainable Chem. Eng.* **2019,** *7*, 10516-10532.

59. Shaplov, A. S.; Ponkratov, D. O.; Vlasov, P. S.; Lozinskaya, E. I.; Malyshkina, I. A.; Vidal, F.; Aubert, P.-H.; Armand, M.; Vygodskii, Y. S. Solid-state electrolytes based on ionic network polymers. *Polym. Sci. Ser. B* **2014,** *56*, 164–177.

60. Shaplov, A. S.; Ponkratov, D. O.; Vlasov, P. S.; Lozinskaya, E. I.; Gumileva, L. V.; Surcin, C.; Morcrette, M.; Armand, M.; Aubert, P.-H.; Vidal, F.; Vygodskii, Y. S. Ionic semi-interpenetrating networks as a new approach for highly conductive and stretchable polymer materials. *J. Mater. Chem. A* **2015,** *3*, 2188-2198.

61. Juger, J.; Vancaeyzeele, C.; Plesse, C.; Nguyen, G. M. T.; Ribeiro, F. B.; Teyssié, D.; Vidal, F. Polymeric ionic liquid based interpenetrating polymer network for all-solid self-standing polyelectrolyte material. *Eur. Polym. J.* **2018,** *106*, 257-265.

62. Li, Y.; Sun, Z.; Shi, L.; Lu, S.; Sun, Z.; Shi, Y.; Wu, H.; Zhang, Y.; Ding, S. Poly(ionic liquid)-polyethylene oxide semi-interpenetrating polymer network solid electrolyte for safe lithium metal batteries. *Chem. Eng. J.* **2019,** *375*, 121925.

63. Li, X.; Zheng, Y.; Pan, Q.; Li, C. Y. Polymerized ionic liquid-containing interpenetrating network solid polymer electrolytes for all-solid-state lithium metal batteries. *ACS Appl. Mater. Interfaces* **2019,** *11*, 34904-34912.

64. Pinaud, J.; Vignolle, J.; Gnanou, Y.; Taton, D. Poly(N-heterocyclic-carbene)s and their CO_2 adducts as recyclable polymer-supported organocatalysts for benzoin condensation and transesterification reactions. *Macromolecules* **2014,** *44*, 1900-1908.

65. Lenz, R. W. Characterization of thermotropic liquid crystalline polymers. *Pure Appl. Chem.* **1985,** *57*, 977-984.

66. Stacey, E. W.; Gainaru, C. P.; Gobet, M.; Wojnarowska, Z.; Bocharova, V.; Greenbaum, S. G.; Sokolov, A. P. Fundamental limitations of ionic conductivity in polymerized ionic liquids. *Macromolecules* **2018,** *51*, 8637-8645.

67. Shen, C.; Zhao, Q.; Evans, C. M. Ion Specific, Odd-even glass transition temperatures and conductivities in precise network polymerized ionic liquids. *Mol. Syst. Des. Eng.* **2019,** *4*¸332-341.

68. Evans, C. M.; Sanoja, G. E.; Popere, B. C.; Segalman, R. A. Anhydrous proton transport in polymerized ionic liquid block copolymers: Roles of block length, ionic content, and confinement. *Macromolecules* **2016,** *49*, 395-404.

69. Choi, U. H.; Middleton, L. R.; Soccio, M.; Buitrago, C. F.; Aitken, H.; Masser, H.; Wagener, K. B.; Winey, K. I.; Runt, J. Dynamic of precise ethylene ionomers containing ionic liquid functionality. *Macromolecules* **2015,** *48*, 410-420.